

Chapter 3

Bohr model of hydrogen



Figure 3.1: Democritus

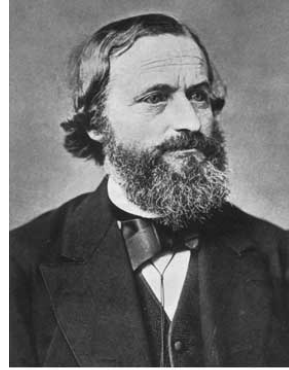
The atomic theory of matter has a long history, in some ways all the way back to the ancient Greeks (Democritus - ca. 400 BCE - suggested that all things are composed of indivisible “atoms”). From what we can observe, atoms have certain properties and behaviors, which can be summarized as follows: Atoms are small, with diameters on the order of 0.1 nm. Atoms are stable, they do not spontaneously break apart into smaller pieces or collapse. Atoms contain negatively charged electrons, but are electrically neutral. Atoms emit and absorb electromagnetic radiation. Any successful model of atoms must be capable of describing these observed properties.



(a) Isaac Newton



(b) Joseph von Fraunhofer



Library of Congress

(c) Gustav Robert Kirchhoff

3.1 Atomic spectra

Even though the spectral nature of light is present in a rainbow, it was not until 1666 that Isaac Newton showed that white light from the sun is composed of a continuum of colors (frequencies). Newton introduced the term “spectrum” to describe this phenomenon. His method to measure the spectrum of light consisted of a small aperture to define a point source of light, a lens to collimate this into a beam of light, a glass spectrum to disperse the colors and a screen on which to observe the resulting spectrum. This is indeed quite close to a modern spectrometer! Newton’s analysis was the beginning of the science of spectroscopy (the study of the frequency distribution of light from different sources).

The first observation of the discrete nature of emission and absorption from atomic systems was made by Joseph Fraunhofer in 1814. He noted that when sufficiently dispersed, the spectrum of the sun was not continuous, but was actually missing certain colors as depicted in Fig. 3.2. These appeared as dark lines in the otherwise continuous spectrum, now known as Fraunhofer lines. (These lines were observed earlier (1802) by William H. Wollaston, who did not attach any significance to them.) These were the first spectral lines to be observed. Fraunhofer made use of them to determine standards for comparing the dispersion of different types of glass. Fraunhofer also developed the diffraction grating to enable not only greater angular dispersion of light, but also standardized measures of wavelength. The latter could not be achieved using glass prisms since the dispersion depended on the type of glass used, which was difficult to make uniform. With this, he was able to directly measure the wavelengths of spectral lines. Fraunhofer’s achievements are all the more impressive, considering that he

died at the early age of 39.

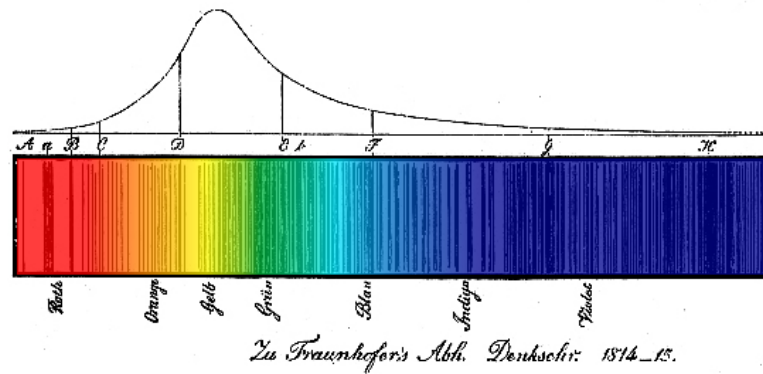


Figure 3.2: Fraunhofer spectrum of the sun. Note the dark lines in the solar spectrum.

The origin of the solar spectral lines were not understood at the time though. It was not until 1859, when Gustav Kirchoff and Robert Bunsen, realized that the solar spectral lines were due to absorption of light by particular atomic species in the solar atmosphere. They noted that several Fraunhofer lines coincided with the characteristic emission lines observed in the spectra of heated elements. By realizing that each atom and molecule has its own characteristic spectrum, Kirchoff and Bunsen established spectroscopy as a tool for probing atomic and molecular structure.

There are two ways in which one can observe spectral lines from an atomic species. The first is to excite the atoms and examine the light that is emitted. Such emission spectra consist of many bright “lines” in a spectrometer, as depicted in Fig. 3.3. The second approach is to pass white light with a continuous spectrum through a glass cell containing the atomic species (in gas form) that we wish to interrogate and observe the absorbed radiation. This absorption spectrum will contain dark spectral lines where the light has been absorbed by the atoms in our cell, illustrated in Fig. 3.3. Note that the number of spectral lines observed by absorption is less than those found through emission.

The road to understanding the origins of atomic spectral lines began with a Swiss schoolmaster by the name of Johann Balmer in 1885, who was trying to understand the spectral lines observed in emission from hydrogen. He noticed that there were regularities in the wavelengths of the emitted lines and found that he could determine the wavelengths with the following

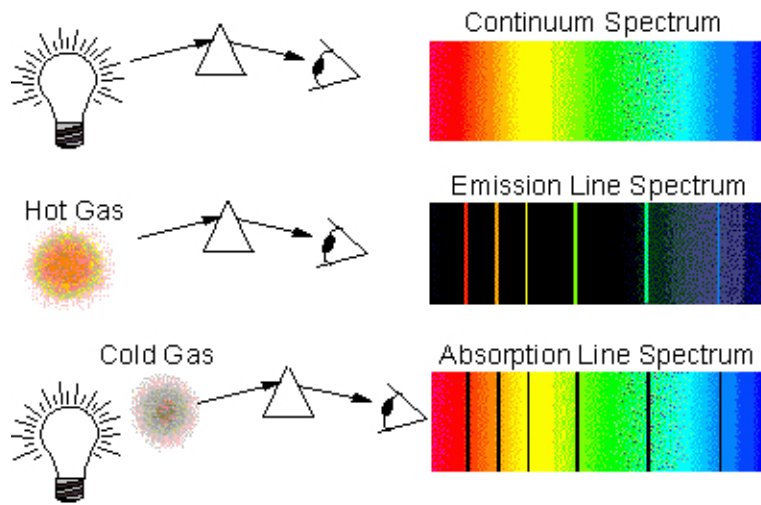


Figure 3.3: Spectra from various experimental setups demonstrating emission and absorption spectra. Spectrum from a white light source (top). Emission spectrum from a hot atomic gas vapor (could also be electrically excited). Absorption spectrum observed when white light is passed through a cold atomic gas.

formula

$$\lambda = \lambda_0 \left(\frac{1}{4} - \frac{1}{n^2} \right)^{-1}, \quad (3.1)$$

where n is an integer greater than two, and λ_0 is a constant length of 364.56 nm. This empirical result was generalized by Johannes Rydberg in 1900 to describe all of the observed lines in hydrogen by the following formula

$$\lambda = \left(\frac{R}{hc} \right)^{-1} \left(\frac{1}{m} - \frac{1}{n^2} \right)^{-1}, \quad (3.2)$$

where m and n are integers ($m < n$), R is known as the Rydberg constant ($R = 13.6$ eV), h is Planck's constant (6.626×10^{-34} Js) and c is the speed of light in vacuum. Although a concise formula for predicting the emission wavelengths for hydrogen were known, there was no physical description for the origin of these discrete lines. The leading theory of the day was that atoms and molecules had certain resonance frequencies at which they would emit, but there was no satisfactory description of the physical origins of these resonances. Furthermore, there were no other closed formulae to predict the emission spectral lines of other, more complex, materials. To take the next steps in understanding these questions required a model of the atom from which the radiation is emitted or absorbed.

3.2 Thomson's plumb-pudding model



(a) Joseph John Thomson

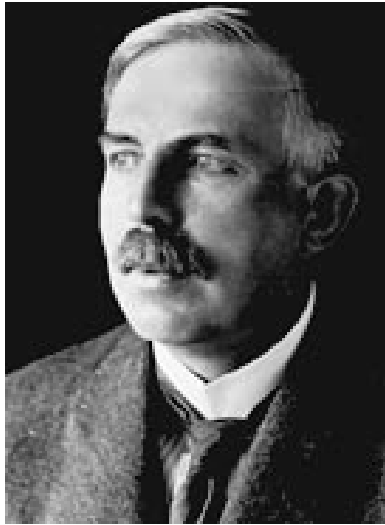


(b) Cartoon of the plum-pudding model of the atom put forth by Thomson.

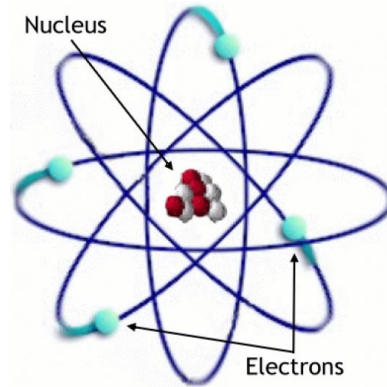
Modern atomic theory has its roots at the end of the 19th century. Atoms were thought to be the smallest division of matter until J. J. Thomson discovered the electron in 1897, which occurred while studying so-called cathode rays in vacuum tubes. He discovered that the rays could be deflected by an electric field, and concluded that these rays rather than being composed of light, must be composed of low-mass negatively charged particles he called corpuscles, which would become known as electrons. Thomson posited that corpuscles emerged from within atoms, which were composed of these corpuscles surrounded by a sea of positive charge to ensure that the atoms were electrically neutral. Thomson's model became known as the plum-pudding model, since the electrons (corpuscles) were embedded in a continuum of positive charge like plums in a plum pudding. Thomson and his students spent a significant amount of effort in attempting to use this model of an atom to calculate the emission and absorption expected from such a charge distribution. However, this model had several holes in it (no pun intended), that could not accurately describe observed emission or absorption spectra, and more significantly, scattering of charged particles from atoms.

3.3 Rutherford's planetary model

In 1909, Hans Geiger and Ernest Marsden carried out a series of experiments to probe the structure of atoms under the direction of Ernest Rutherford at the University of Manchester. The experiment, often called the gold-foil experiment, sent a beam of positively charged particles, called α particles



(a) Ernest Rutherford



(b) Pictorial representation of the Rutherford (or planetary) model of an atom, in which the positively charged nucleus, which contains the majority of the atomic mass, is surrounded by orbiting electrons.

(now known to be ionized helium atoms) onto a thin gold foil sheet, as sketched in Fig. 3.4. If Thomson's plum-pudding model were correct, the α particles should have passed through the foil with only minor deflection. This is because the α particles have a significant mass, and the charge in the plum-pudding model of the atom is spread widely throughout the atom. However, the results were quite surprising. Many of the α particles did pass through with little change to their path. However they observed that a small fraction of particles were deflected through angles much larger than 90° .

Rutherford analyzed the scattering data and developed a model based on a the positive charge of the atom, localized in a small volume, containing the majority of the atomic mass. This is summarized in his words

It was quite the most incredible event that has ever happened to me in my life. It was almost as incredible as if you fired a 15-inch shell at a piece of tissue paper and it came back and hit you. On consideration, I realized that this scattering backward must be the result of a single collision, and when I made calculations I saw that it was impossible to get anything of that order of magnitude unless you took a system in which the greater part of the mass of the atom was concentrated in a minute nucleus. It was then that I had the idea of an atom with a minute massive center, carrying a charge.

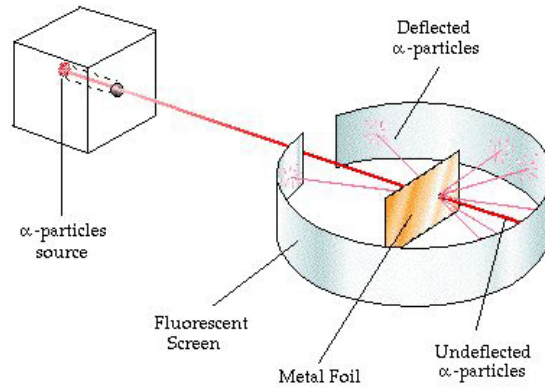


Figure 3.4: Depiction of the gold-foil experiment in which α particles are scattered from a thin gold film and observed on a fluorescent screen.

- Ernest Rutherford

In 1911, Rutherford proposed that the positive charge of an atom was concentrated in a small central volume, which also contained the bulk of the atomic mass. This “nucleus” is surrounded by the negatively charged electrons as illustrated in Fig. 3.4b. Thus the Rutherford, or planetary, model of the atom came into being.

Classical discussion of nuclear atom The classical description of the nuclear atom is based upon the Coulomb attraction between the positively charged nucleus and the negative electrons orbiting the nucleus. To simplify the discussion, we focus on the hydrogen atom, with a single proton and electron. Furthermore, we consider only circular orbits. The electron, with mass m_e and charge $-e$ moves in a circular orbit of radius r with constant tangential velocity v . The attractive Coulomb force provides the centripetal acceleration v^2/r to maintain orbital motion. (Note we neglect the motion of the nucleus since its mass is much greater than the electron.) The total force on the electron is thus

$$F = \frac{1}{4\pi\epsilon_0} \frac{e^2}{r^2} = \frac{m_e v^2}{r}, \quad (3.3)$$

where $\epsilon_0 = 8.854 \times 10^{-12}$ F/m is the permittivity of free space. Note that this is positive since we are taking the force to be acting in the $-\hat{\mathbf{r}}$ direction, where $\hat{\mathbf{r}}$ is the unit vector pointing from the nucleus to the electron position (this cancels out the - sign from the electron charge). From this equation, we can determine the kinetic energy of the electron (neglecting relativistic effects)

$$K = \frac{1}{2} m_e v^2 = \frac{1}{8\pi\epsilon_0} \frac{e^2}{r}. \quad (3.4)$$

The potential energy of the electron is just given by the Coulomb potential

$$U = -\frac{1}{4\pi\epsilon_0} \frac{e^2}{r}. \quad (3.5)$$

Here the potential energy is negative due to the sign of the electron charge. The total energy $E = K + U$ is thus

$$E = -\frac{1}{8\pi\epsilon_0} \frac{e^2}{r}. \quad (3.6)$$

Up to this point we have neglected a significant aspect of classical physics. A major challenge for the classical treatment of the planetary model of the atom stems from the fact that the atomic nucleus and orbiting electrons carry net charges, whereas the Sun and planets of the solar system are electrically neutral. It is well known that oscillating charges will emit electromagnetic radiation, and thus carry away mechanical energy. Then according to the classical theory of the atom the electron will spiral into the nucleus in only a matter of microseconds, all the while continually emitting radiation. Furthermore, as the electron spirals in towards the nucleus the frequency of emitted radiation increases continuously, owing to the increased frequency of oscillation. Clearly these are not observed - atoms are stable, do not continually emit radiation, and do not emit a continuous spectrum of radiation. Although this model, based upon classical physics in which the electrons were held to the nucleus through the Coulomb force, could not satisfactorily describe the observed atomic spectra, the concept of a nuclear atom would play a central role in developing a theory that would do so.

3.4 Bohr's model

In 1911, fresh from completion of his PhD, the young Danish physicist Niels Bohr left Denmark on a foreign scholarship headed for the Cavendish Laboratory in Cambridge to work under J. J. Thomson on the structure of atomic systems. At the time, Bohr began to put forth the idea that since light could no longer be treated as continuously propagating waves, but instead as discrete energy packets (as articulated by Planck and Einstein), why should the classical Newtonian mechanics on which Thomson's model was based hold true? It seemed to Bohr that the atomic model should be modified in a similar way. If electromagnetic energy is quantized, i.e. restricted to take on only integer values of $h\nu$, where ν is the frequency of light, then it seemed reasonable that the mechanical energy associated with the energy of atomic electrons is also quantized. However, Bohr's still somewhat vague ideas were not well received by Thomson, and Bohr decided to move from Cambridge after his first year to a place where his concepts about quantization of electronic motion in atoms would meet less opposition. He chose



Figure 3.5: Niels Henrik David Bohr

the University of Manchester, where the chair of physics was held by Ernest Rutherford. While in Manchester, Bohr learned about the nuclear model of the atom proposed by Rutherford.

To overcome the difficulty associated with the classical collapse of the electron into the nucleus, Bohr proposed that the orbiting electron could only exist in certain special states of motion - called *stationary states*, in which no electromagnetic radiation was emitted. In these states, the angular momentum of the electron L takes on integer values of Planck's constant divided by 2π , denoted by $\hbar = h/2\pi$ (pronounced h-bar). In these stationary states, the electron angular momentum can take on values $\hbar, 2\hbar, 3\hbar, \dots$, but never non-integer values. This is known as *quantization of angular momentum*, and was **one of Bohr's key hypotheses**. Note that this differs from Planck's hypothesis of energy quantization, but as we will see it does lead to quantization of energy.

For circular orbits, the position vector of the electron \mathbf{r} is always perpendicular to its linear momentum \mathbf{p} . The angular momentum $\mathbf{L} = \mathbf{r} \times \mathbf{p}$ has magnitude $L = rp = m_e v r$ in this case. Thus Bohr's postulate of quantized angular momentum is equivalent to

$$m_e v r = n \hbar, \quad (3.7)$$

where n is a positive integer. This can be solved to give the velocity

$$v = \frac{n \hbar}{m_e r}. \quad (3.8)$$

Using this result in Eq. (3.3),

$$\frac{m_e v^2}{r} = \frac{m_e}{r} \left(\frac{n\hbar}{m_e r} \right)^2 = \frac{1}{4\pi\epsilon_0} \frac{e^2}{r^2}, \quad (3.9)$$

we find a series of allowed radii

$$r_n = \frac{4\pi\epsilon_0\hbar^2}{m_e e^2} n^2 = a_0 n^2. \quad (3.10)$$

Here $a_0 = 0.0529$ nm is known as the Bohr radius. Equation (3.10) gives the allowed radii for electrons in circular orbits of the hydrogen atom.

This is a significant and unexpected result when compared to the classical behavior discussed previously. A satellite in a circular orbit about the earth can be placed at any altitude (radius) by providing an appropriate tangential velocity. However, electrons are only allowed to occupy orbits with certain discrete radii. Furthermore, this places constraints to the allowed velocity, momentum, and total energy of the electron in the atom. By using Eq. (3.10) we can find the allowed velocity, momentum, and total energy in hydrogen are given by

$$v_n = \frac{\hbar}{m_e a_0 n}, \quad (3.11)$$

for the quantized velocity,

$$p_n = \frac{\hbar}{a_0 n}, \quad (3.12)$$

for the quantized momentum (note we assume nonrelativistic momentum), and

$$E_n = -\frac{m_e e^4}{32\pi^2 \epsilon_0^2 \hbar^2} \frac{1}{n^2} = -\frac{e^2}{8\pi\epsilon_0 a_0} \frac{1}{n^2} = -\frac{E_1}{n^2}, \quad (3.13)$$

for the quantized energy levels. Here $E_1 = 13.6$ eV is the ground state energy of the system.

The energy levels are indicated schematically in Fig. 3.6. The electron energy is quantized, with only certain discrete values allowed. In the lowest energy level, known as the ground state, the electron has energy $E_1 = 13.6$ eV. The higher states, $n = 2, 3, 4, \dots$ with energies -3.6 eV, -1.5 eV, -0.85 eV, \dots are called excited states. The integer, n that labels both the allowed radius and energy level, is known as the *principle quantum number* of the atom. It tells us what energy level the electron occupies.

When the electron and nucleus are separated by an infinite distance ($n \rightarrow \infty$) we have $E = 0$. By bringing the electron in from infinity to a particular state n , we release energy $E = -(E_{\text{final}} - E_{\text{initial}}) = |E_n|$ (note the minus sign comes from the energy being released). Similarly, if we start with an atom in state n , we must supply at least $|E_n|$ to free the electron. This energy is known as the *binding energy* of the state n . If we supply more

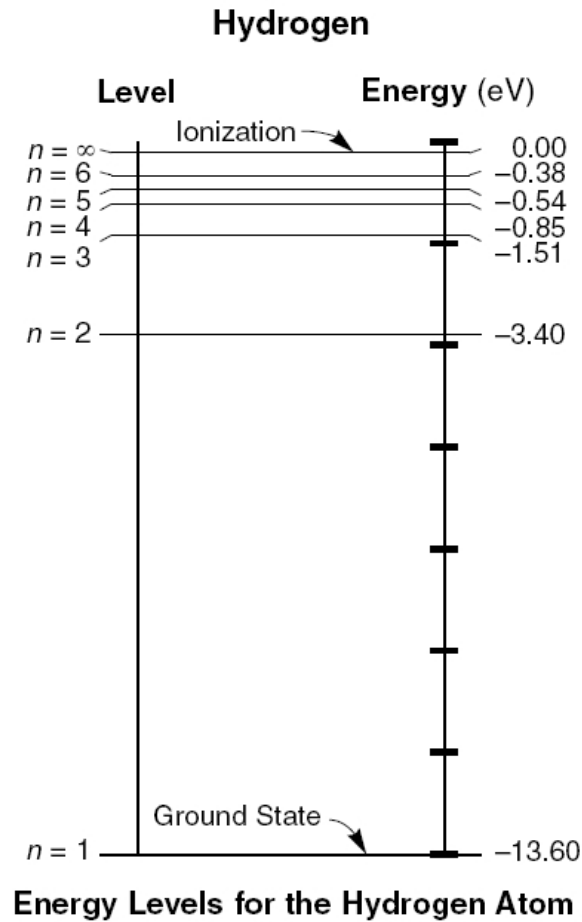


Figure 3.6: Schematic representation of the discrete allowed energy levels in the hydrogen atom.

energy than $|E_n|$ to the electron, then the excess beyond the binding energy will appear as kinetic energy of the freed electron.

The *excitation energy* of an excited state n is the energy above the ground state, $E_n - E_1$. For the first excited state, $n = 2$, the excitation energy is

$$\Delta E = E_2 - E_1 = -3.4 \text{ eV} - (-13.6 \text{ eV}) = 10.2 \text{ eV}. \quad (3.14)$$

Once Bohr had worked out that the energy levels of hydrogen were quantized, i.e. only allowed to take on discrete values, he was able to easily describe the spectral lines observed for hydrogen if he were to posit a second postulate: radiation can only be emitted when the atom makes a transition from one energy level, say n , to another with lower energy, $m < n$. The energy of the emitted photon will thus be given by the difference in energy between these two levels

$$E_{\text{ph}} = E_m - E_n = E_1 \left(\frac{1}{m^2} - \frac{1}{m^2} \right). \quad (3.15)$$

Using Planck's relation between energy and frequency, $E = h\nu$, we can see that the expected frequency spectral lines are

$$\nu = \frac{E_1}{h} \left(\frac{1}{m^2} - \frac{1}{m^2} \right), \quad (3.16)$$

or in terms of wavelength

$$\lambda = \frac{hc}{E_1} \left(\frac{1}{m^2} - \frac{1}{m^2} \right)^{-1}. \quad (3.17)$$

Comparison of this with Rydberg's empirical formula, Eq. (1.2), Bohr identified his ground state energy value, $E_1 = 13.6$ eV with the experimentally determined Rydberg constant, $R = 13.6$ eV. These two agreed well within experimental errors of the time.

Note that Bohr's second postulate, i.e. the energy of an emitted photon from an atom is given by the difference in energy level, contradicts the concepts of classical physics in which an oscillating charge emits radiation at its frequency of oscillation. For an electron in state n with energy E_n , its oscillation frequency is just $\nu_n = E_n/h$. Taken together, Bohr's postulates can be summarized as follows

Bohr's postulates

- Quantized angular momentum: $L = m_e v r = n\hbar$.
- Radiation is only emitted when an atom makes transitions between stationary states: $E_{\text{ph}} = E_m - E_n$.

By examining Eq. (3.12), we see that this can be rewritten as

$$\frac{h}{p_n} = 2\pi a_0 n = \frac{2\pi r_n}{n}. \quad (3.18)$$

As we will see when we discuss the wave nature of matter and the de Broglie wavelength, the quantization of angular momentum, which leads to allowed orbits with radii $r_n = a_0 n^2$ and momenta $p_n = \hbar/a_0 n = \hbar n/r_n$ implies that the circumference of the allowed states is an integer multiple of the de Broglie wavelength $\lambda_{\text{dB}} = h/p$

$$n\lambda_{\text{dB}} = 2\pi r_n \quad (3.19)$$

which follows easily from Eq. (3.18) above.

Hydrogen-like ions

The treatment of hydrogen atoms prescribed by Bohr can be generalized to describe the energy level structure and electromagnetic radiation spectra of *hydrogen-like* ions, i.e. a positive nucleus with charge Ze (Z the integer number of protons in the nucleus) orbited by a *single* electron. The nuclear charge comes into the Bohr model in only one place - the Coulomb force acting on the electron, Eq. (3.3), which becomes

$$F = \frac{1}{4\pi\epsilon_0} \frac{Ze^2}{r^2} = \frac{m_e v^2}{r}. \quad (3.20)$$

The method applied by Bohr is the same as before, but with e^2 replaced by Ze^2 . This results in a new expression for the allowed radii

$$r_n = \frac{4\pi\epsilon_0 \hbar^2}{m_e Ze^2} n^2 = \frac{a_0 n^2}{Z}, \quad (3.21)$$

and allowed energy levels

$$E_n = -\frac{m_e (Ze^2)^2}{32\pi^2 \epsilon_0^2 \hbar^2} \frac{1}{n^2} = -\frac{Z^2 e^2}{8\pi\epsilon_0 a_0} \frac{1}{n^2} = -E_1 \frac{Z^2}{n^2}. \quad (3.22)$$

The orbits with high- Z atoms are closer to the nucleus and have larger (more negative) energies, i.e. they are more tightly bound to the nucleus. The frequencies of emitted radiation from such an ion will also be modified, and from Eq. (3.22) we see this should scale with Z^2

$$\nu = \frac{E_1 Z^2}{h} \left(\frac{1}{m^2} - \frac{1}{m'^2} \right), \quad (3.23)$$

or in terms of wavelength

$$\lambda = \frac{hc}{E_1 Z^2} \left(\frac{1}{m^2} - \frac{1}{m'^2} \right)^{-1}. \quad (3.24)$$

Absorption spectra

The Bohr model not only helps us to understand the emission spectrum of atoms, but also explain why atoms do not absorb at all the same wavelengths that it emits. Isolated atoms are normally found in the ground state - excited states live for very short time periods (≈ 1 ns) before decaying to the ground state. The absorption spectrum therefore contains only transitions from the ground state ($n = 1$). To observe transitions from the first excited state ($n = 2$) would require a significant number of atoms to occupy this state initially. Assuming that the atoms are excited by their thermal energies,

this implies that to excite an atom to the first excited state from the ground state requires temperature that satisfies

$$k_{\text{B}}T = E_2 - E_1 = 10.2 \text{ eV},$$

which gives a temperature

$$T = \frac{(10.2 \text{ eV})(1.6 \times 10^{-19} \text{ J/eV})}{1.38 \times 10^{-23} \text{ J/K}} \approx 1.2 \times 10^5 \text{ K},$$

which is much larger than room temperature (the surface of the sun has temperature $T \approx 6 \times 10^3 \text{ K}$).

3.5 Franck-Hertz experiment



(a) James Franck



(b) Gustav Ludwig Hertz

Less than a year after Bohr published his first papers describing his theory of the structure of hydrogen and its corresponding spectrum, further evidence for the Bohr model was provided by German physicists James Franck and Gustav Ludwig Hertz (nephew of Heinrich Rudolf Hertz of electromagnetic waves and photoelectric effect fame). They set out to experimentally probe the energy level structure of atoms by colliding an atomic vapor with a stream of electrons. The experiment (for which they were awarded the Nobel Prize in 1925) that they performed, now known as the Franck-Hertz experiment, is depicted in Fig. 3.7 below. A filament (F) heats a cathode (C) from which electrons are emitted. The electrons are accelerated towards a metal grid (G) by a variable potential difference V . Some of the electrons can pass through the mesh in the grid and reach the collection plate (P)

if the accelerating potential V exceeds a small retarding potential V_0 . The current between the cathode and collection plate i is measured by an ammeter (A). The filament, cathode, grid, and collection plate are enclosed in a vacuum tube to ensure that the electrons do not collide with any molecules in the atmosphere.

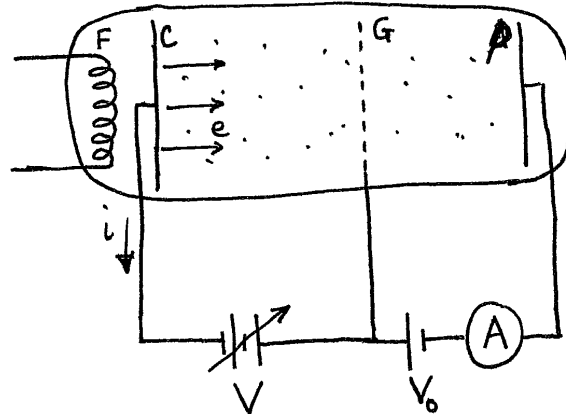


Figure 3.7: Franck-Hertz experimental setup. Electrons freed from the cathode (C) by heating from a filament (F) are accelerated by voltage V toward a grid (G). For $V > V_0$, the electrons are collected on a plate (P) and registered using an ammeter (A). Collisions with atoms can be either elastic or inelastic.

To probe an atomic species, Franck and Hertz introduced a low-pressure atomic gas (they used mercury) into the tube. As the accelerating voltage is increased from zero more and more electrons reach the collection plate and a steadily increasing current is observed, as shown in Fig. 3.8. The electrons can make collisions with the atoms in the tube, but they will lose no energy since the collisions are perfectly elastic - only their direction of propagation can change. If this were the only possible way for the electrons and atoms to interact, then one would expect a continuously increasing current. However, this is not what was observed as shown in Fig. 3.8. When the accelerating voltage reaches approximately integer values of 4.9 V, a sharp drop in the measured current is observed, implying that a significant number of electrons have lost much of their kinetic energy.

To interpret their results, Franck and Hertz suggested that the only way an electron can lose energy in a collision is if the electron has sufficient energy to cause the atom to make a transition to an excited state. Thus, when the energy of electrons just reaches the transition energy between the ground and first excited state (assuming all atoms start in the ground state) $\Delta E = E_1 - E_2$ (for hydrogen this is 10.2 eV, while for mercury it is 4.9 eV), the electrons can make an *inelastic collision* with the atom,

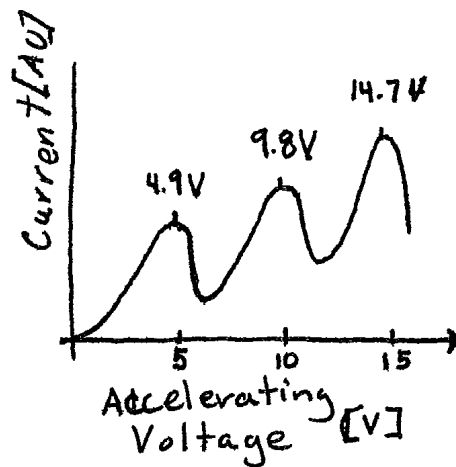


Figure 3.8: Franck-Hertz experimental results with mercury vapor. As the accelerating voltage is increased, the measured current passing through the gas increases until the transition energy between the ground state and first excited state 4.9 eV, is reached. Electrons will undergo inelastic collisions at this energy, giving up their kinetic energy to excited the mercury atom and thus have insufficient energy to reach the collection plate. At higher acceleration voltages, the electrons can undergo multiple collisions, each time giving up energy 4.9 eV.

leaving ΔE energy with the atom, which is now in the $n = 2$ excited state, and the original electron is scattered with very little energy remaining. As the accelerating voltage is increased, we begin to see the effects of multiple collisions. That is, when $V = 9.8$ V the electrons have sufficient energy to collide with two different atoms, losing energy of 4.9 eV in each collision. This clearly demonstrates the existence of atomic excited states with discrete energy values. Indeed, in the emission spectrum of mercury, an intense ultraviolet spectral line with wavelength 254 nm, corresponding to energy 4.9 eV, is observed. The Franck-Hertz experiment showed that an electron must have a minimum amount of energy to make an inelastic collision with an atom, which we now interpret as the energy required to transition to an excited state from the ground state.

3.6 Deficiencies of the Bohr model

In spite of the successes of the Bohr model to predict the spectra of hydrogen, and hydrogen-like ions, there are several results that it cannot explain. It cannot be applied to atoms with two or more electrons since it does not take into account the Coulomb interaction between electrons. A closer look at the atomic spectral lines emitted from various gases shows that some spectral

“lines” are in fact not single lines, but a pair of closely spaced spectral lines (known as doublets). These closely spaced lines are known as *fine structure*. Furthermore, the model does not allow us to calculate the relative intensities of the spectral lines.

More serious deficiencies in the Bohr model is that it predicts the incorrect value of angular momentum for the electron! For the ground state of hydrogen ($n = 1$), the Bohr theory gives $L = \hbar$, while experiment clearly shows $L = 0$.

Furthermore, as we will see in the next chapter, the Bohr model violates the Heisenberg uncertainty relation. In Bohr’s defense, his theory was developed more than a decade before the advent of wave mechanics and the introduction of the uncertainty principle. The uncertainty relation $\Delta x \Delta p_x \gtrsim \hbar$ is valid for any direction in space. Choosing the radial direction in the atom, this becomes $\Delta r \Delta p_r \gtrsim \hbar$. For an electron moving in a circular orbit, we know its radius exactly and thus $\Delta r = 0$. However, since it is moving in a circular orbit, it cannot have any radial velocity, and thus $p_r = 0$ and $\Delta p_r = 0$. This simultaneous exact knowledge of both r and p_r violates the uncertainty principle.

These problems associated with the Bohr model can be summarized as follows.

Deficiencies of the Bohr model

- Cannot be applied to multi-electron atoms.
- Does not predict fine structure of atomic spectral lines.
- Does not provide a method to calculate relative intensities of spectral lines.
- Predicts the wrong value of angular momentum for the electron in the atom.
- Violates the Heisenberg uncertainty principle (although Bohr’s model preceded this by more than a decade)

As with classical physics, we do not wish to discard the Bohr model of the atom, but rather make use of it in its realm of applicability, and in guiding our intuition to develop further models of atomic structure. The Bohr model gives us a helpful picture of atomic structure that can describe properties of atoms. For example, many properties associated with magnetism can be understood through Bohr orbits. Furthermore, as you will find next year when you study the hydrogen atom using the Schrödinger equation, the energy levels are exactly the same as those given by the Bohr model.

Chapter 4

Wavelike properties of particles

The framework of mechanics used to describe quantum systems is often called “wave mechanics” owing to the wave-like behavior that can be observed for what would classically be described by a particle trajectory. In this chapter we discuss experimental evidence of wave-like phenomena associated with particles such as electrons. In this discussion you will notice the terms *probability* of a measurement outcome, the *average* of many repeated measurements, and the *statistical* behavior of a system. These terms are an integral part of quantum physics. The classical notions of a fixed particle trajectory and certainty of measurement outcomes do not hold for quantum systems and the quantum ideas of probability and statistically distributed measurement outcomes take rein.

4.1 de Broglie waves

We begin by introducing the concept of “matter waves”. Previously, when discussing the photoelectric effect and Compton scattering, we saw that these experiments could be explained by using a particle-like description of light. However, the double-slit experiment, in which two identical slits are illuminated and an interference pattern is recorded on a screen far from the slit, requires a wave description. Upon closer inspection the double-slit experiment does show some particle-like properties of light as well though. At low light levels, only individual photons are registered at point-like positions on the observation screen (as depicted in Fig. 4.2. The interference pattern is not initially present on the screen, and only appears after a finite time period required to collect sufficient number of photons. The wave properties of light are shown in the collective interference pattern observed after many photons have been detected. However, the particle properties of light are illustrated on a shot-by-shot basis - each photon appears as a point-like



Figure 4.1: Louis de Broglie

detection event on the screen. We see that wave and particle properties are present in such an experiment. This idea that a quantum system possesses both wave and particle properties, is known as *wave-particle duality*.

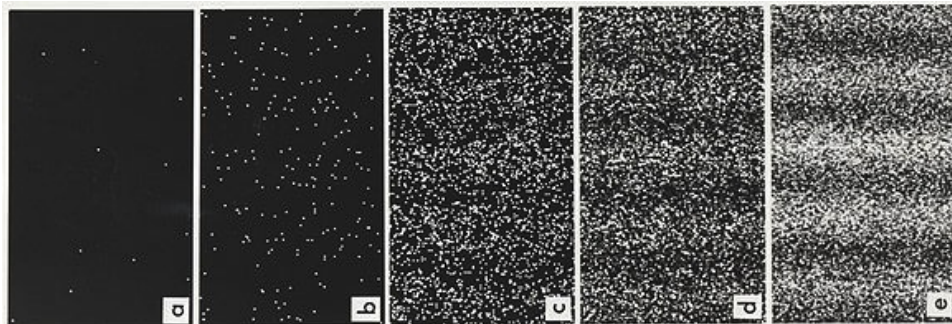


Figure 4.2: The build up of a double-slit interference pattern showing individual particle detection. The number of detected electrons is (a) 11, (b) 200, (c) 6000, (d) 40000, and (e) 140000.

In 1924 Louis de Broglie (pronounced “de Broy”) put forth a significantly new concept regarding the behavior of quantum systems in his PhD thesis. While contemplating the wave-particle duality of light, he questioned whether this dual particle-wave nature is a property of light only, but rather applies to all physical systems as well? He chose to suggest the latter, that all physical systems should demonstrate this wave-particle duality. Special relativity implies that

$$E^2 = (cp)^2 + (mc^2)^2, \quad (4.1)$$

which can be simplified for a photon (zero rest mass) to yield,

$$E = cp. \quad (4.2)$$

Using the Planck relationship between energy and frequency, $E = h\nu$, or in terms of the wavelength, $E = hc/\lambda$, we arrive at the following relationship between wavelength and momentum for a photon

$$\lambda_{\text{dB}} = \frac{h}{p}, \quad (4.3)$$

De Broglie went further and suggested that this relationship holds for material systems as well as light. That is, a material system with momentum p has associated with it a wave of wavelength λ_{dB} given by Eq. (4.3) above.

De Broglie waves and the Bohr model

If we examine the resulting effects de Broglie's hypothesis has on the Bohr model of hydrogen, we first recall that the allowed radii for the Bohr model are given by

$$r_n = a_0 n^2, \quad (4.4)$$

where $a_0 \approx 0.5\text{\AA}$ is the Bohr radius and n is a positive integer. The momentum of the photon in state n is given by

$$p_n = \frac{\hbar}{a_0 n}, \quad (4.5)$$

or $p_n = n\hbar/r_n$, where $\hbar = h/2\pi$. Through the de Broglie relation between wavelength and momentum, $\lambda = h/p = h/(n\hbar/r_n) = 2\pi r_n/n$, we see that the circumference of an orbit is equal to an integer number of de Broglie wavelengths

$$2\pi r_n = n\lambda, \quad (4.6)$$

as depicted in Fig. 4.3 below.

De Broglie waves in everyday life?

The de Broglie wavelength for everyday objects is extremely small. For example a cricket ball ($m = 0.16$ kg and velocity $v = 161$ km/hr ≈ 45 m/s) has a de Broglie wavelength

$$\lambda_{\text{cricket}} = \frac{h}{mv} = \frac{6.626 \times \text{eV}}{(0.16 \text{ kg})(45 \text{ m/s})} \approx 9 \times 10^{-35} \text{ m}, \quad (4.7)$$

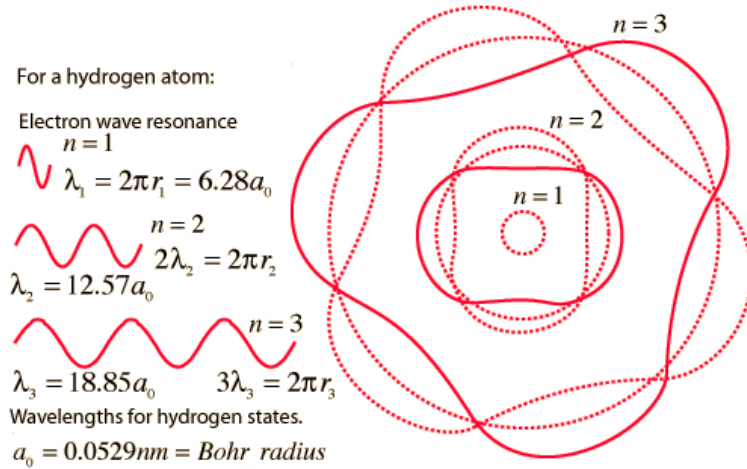


Figure 4.3: Illustration of the relationship between the de Broglie wavelength of electrons in the Bohr model of the hydrogen atom. Only an integer number of de Broglie waves around the circumference of a given Bohr orbit is allowed.

or Usain Bolt ($m = 92 \text{ kg}$ and velocity $v = 45 \text{ km/hr} \approx 12 \text{ m/s}$) has a de Broglie wavelength

$$\lambda_{\text{Bolt}} = \frac{h}{mv} = \frac{6.626 \times 10^{-34} \text{ J s}}{(92 \text{ kg})(12 \text{ m/s})} \approx 6 \times 10^{-37} \text{ m}. \quad (4.8)$$

Suppose we tried to observe the wave-nature of these objects by using a double slit type experiment. The spacing between adjacent fringes in a double-slit experiment is given by $\Delta x = \lambda L/d$, where λ is the wavelength of the incident wave on the slit, d is the spacing between the slits, and L is the distance from the slit to the observation screen. To obtain a reasonable value of fringe separation, say 10^{-6} m requires the ratio of screen distance to slit spacing to be on the order of 10^{28} , which is not feasible. These wavelengths are extremely small compared to anything that can be observed in a modern laboratory. However, if we examine the de Broglie wavelengths associated with electrons or atoms moving at modest (non-relativistic) speeds we find that these are on the same length scale as the spacing of atoms in a crystal lattice. For example, electrons that have been accelerated with a potential difference of 50 V have kinetic energy $K \approx 50 \text{ eV}$ and thus non-relativistic momentum $p = \sqrt{2mK}$, where m is the rest mass of the electron. The associated de Broglie wavelength for such electrons is thus

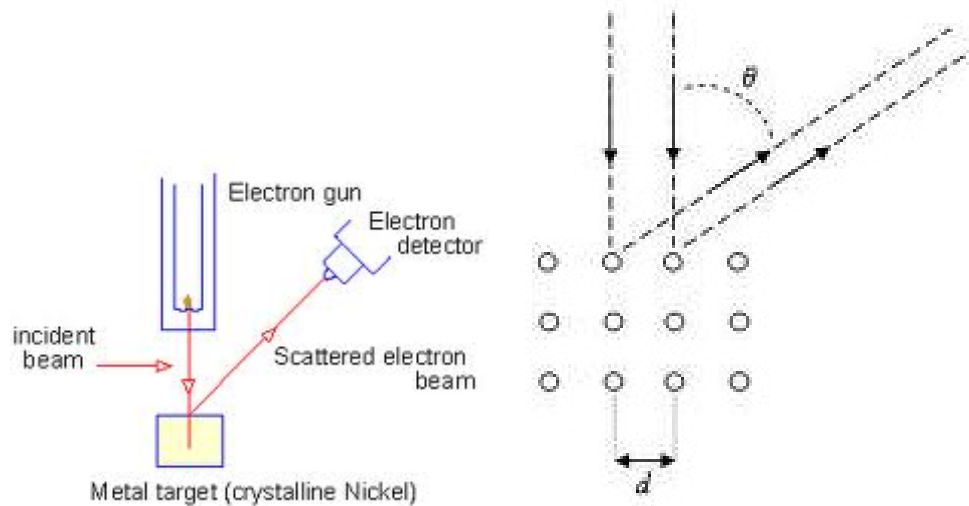
$$\lambda_{\text{dB}} = \frac{hc}{pc} = \frac{hc}{\sqrt{2mc^2K}} = \frac{1240 \text{ eV nm}}{\sqrt{2(0.511 \times 10^6 \text{ eV})(50 \text{ eV})}} = 0.17 \text{ nm}. \quad (4.9)$$

Here I have made use of the numerical values of the product of the Planck

constant and vacuum speed of light $hc \approx 1240 \text{ eV nm}$, and the rest energy of the electron $mc^2 \approx 0.511 \text{ MeV}$, two values I suggested incorporating into your long-term memory. You will find these extremely helpful in performing numerical calculations.

As you can see, it is not feasible to observe the wave properties of macroscopic systems owing to the extremely small de Broglie wavelengths for such objects. However, there is some hope for observing such wave behavior for atomic scale systems as demonstrated by the wavelength for the electrons calculated above.

4.1.1 Davisson-Germer Experiment



(a) Experimental setup: An electron beam incident on a crystalline nickel target is scattered and the scattered electrons are detected by a movable detector at an angle θ with respect to the incident beam. (b) Diffraction scattering geometry in which electrons scatter off the first layer of atoms in the crystal with lattice spacing d at an angle θ .

Figure 4.4: Davisson-Germer experiment.

The first experimental confirmation of the wave-nature of matter and quantitative confirmation of the de Broglie relation, Eq. (4.3), was performed with a beam of electrons. In 1926, at Bell Labs, Clinton Davisson and Lester Germer were investigating the reflection of electron beams from the surface of nickel crystals. A schematic view of their experiment is shown in Fig. 4.4a. A beam of electrons accelerated through a potential difference V is incident on a crystalline nickel target. Electrons are scattered in many directions by the atoms of the crystal and detected at an angle θ from the incident beam. If we assume that each atom in the crystal can act as a scatterer, then the scattered *electron waves* can interfere, and we then have

a crystal diffraction grating for the electrons, as depicted in Fig. 4.4b. Because the electrons had low kinetic energy, they did not penetrate very far into the crystal, making it sufficient to consider only diffraction due to the plane of atoms at the surface. The situation is precisely analogous to the use of a reflection grating for light. The spacing d between atoms on the surface is analogous to the spacing between slits in an optical grating. The diffraction maxima occur when the path length difference between adjacent scatterers (atoms in this case) ($d \sin \theta$) is an integer number of wavelengths ($n\lambda$),

$$d \sin \theta = n\lambda. \quad (4.10)$$

The lattice spacing for nickel is known to be $d = 0.215$ nm. For an accelerating voltage $V = 54$ eV ($\lambda = 0.167$ nm), Davisson and Germer observed a peak in the scattered electrons at an angle $\theta = 50^\circ$ as shown in Fig. 4.5, which corresponds to first-order diffraction from a lattice with spacing $d = \lambda / \sin \theta \approx 0.218$, which is very close to the accepted value for nickel.

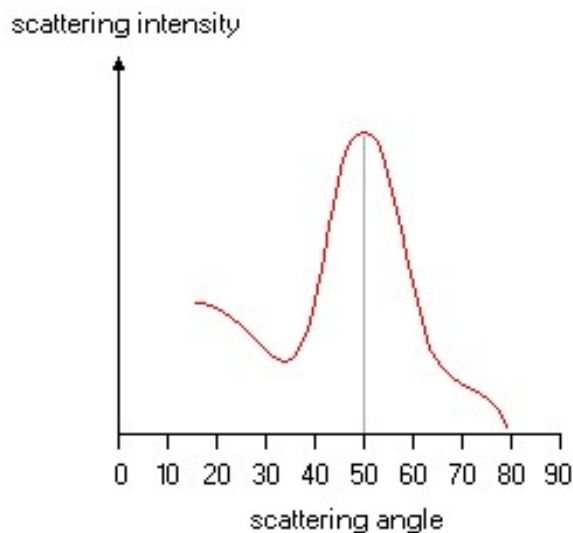


Figure 4.5: Scattering intensity as a function of scattering angle for an electron beam accelerated through 54 V potential incident on crystalline nickel as in the Davisson-Germer experiment.

If there is some uncertainty in the kinetic energy of the particle beam, ΔK , this is translated into uncertainty in the wavelength of the incident de Broglie wavelength $\Delta \lambda$, owing to the relationship between the two, $\lambda = hc / \sqrt{2mc^2 K}$. The uncertainty in wavelength can be found by considering the ratio of “infinitesimal” changes in wavelength to kinetic energy and equating this with the first derivative of wavelength with respect to kinetic energy

$$\frac{\Delta\lambda}{\Delta K} \approx \left| \frac{d\lambda}{dK} \right|, \quad (4.11)$$

and solving for $\Delta\lambda$ to give

$$\Delta\lambda \approx \left| \frac{d\lambda}{dK} \right| \Delta K = \frac{1}{2} \lambda \frac{\Delta K}{K}. \quad (4.12)$$

The fractional uncertainty of the wavelength is thus half the fractional uncertainty of the kinetic energy, i.e.

$$\frac{\Delta\lambda}{\lambda} \approx \frac{1}{2} \frac{\Delta K}{K}. \quad (4.13)$$

Note that for a photon with the same fraction uncertainty in the total energy as the fractional uncertainty in a particle kinetic energy, $\Delta E/E = \Delta K/K$, leads to wavelength fractional uncertainty $\Delta\lambda/\lambda = \Delta E/E$, without the factor of 1/2. This is because the momentum of the photon is directly proportional to the total photon energy, whereas the momentum of the particle (in the non-relativistic regime) is proportional to the square root of the kinetic energy.

The uncertainty in de Broglie wavelength will lead to an uncertainty in constructive interference scattering angle ($\theta \approx n\lambda/d$ in the small angle approximation), and thus a blurring out of the diffraction spot. The uncertainty in the diffraction angle $\Delta\theta$ can be approximated by

$$\frac{\Delta\theta}{\theta} \approx \frac{\Delta\lambda}{\lambda}. \quad (4.14)$$

Thus we see that the diffraction angle uncertainty will be half as small for a beam of non-relativistic particles in comparison with similar photons.

4.2 Double-slit interference and complementarity

The definitive evidence for the wave nature of light is typically attributed to the double-slit experiment performed by Thomas Young in 1801. In principle, it should be possible to perform double-slit experiments with material systems, such as electrons, neutrons, atoms, and even molecules! However, technological difficulties for producing double slits for particles are extremely challenging and only in recent years have these been addressed. The first double-slit experiment with electrons was performed in 1961. Since then, numerous experiments have been performed on a wide variety of systems, including bucky balls and more recently, large organic molecules (see articles by Arndt et al, and Zhao and Schöllkopf linked on website).

Considering double-slit interference of particles, we note that the detection of a particle at a point x on the screen is governed by the interference of

pathways that the particle can take. This is in line with Feynman's multiple path formulation of quantum mechanics for those interested. If we take our double slit setup to be similar to that shown in Fig. 4.6, there are two possible paths the particle can take (r_1 or r_2) to reach point x on the screen, corresponding to the particle passing through slit 1 or 2 respectively. The phases associated with each path is given by the wavenumber $k = 2\pi/\lambda$ multiplied by the pathlength $r_1 = \sqrt{L^2 + (x + d/2)^2}$ or $r_2 = \sqrt{L^2 + (x - d/2)^2}$.

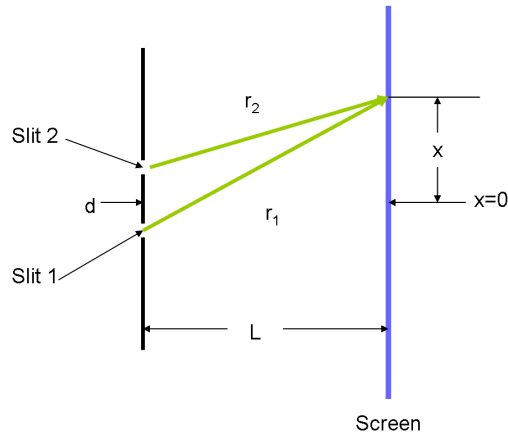


Figure 4.6: Double-slit interference setup. Two slits of negligible width separated by a distance d . The number of particles per unit time (particle flux) at a point x on a collection screen a distance L away from the slits can be calculated by considering the amplitudes for the two possible paths a particle can take r_1 and r_2 .

The particle flux (number of particles per unit time) at a point x on the screen is proportional to the modulus squared of the total amplitude for all possible paths the particle can take to reach x , which for our double slit, there are two A_1 and A_2 . If we assume these paths have equal amplitudes and differ only in the phases, this gives a flux

$$N = |A_{\text{tot}}|^2 = |A_1 + A_2|^2 = A^2 \left| e^{i\phi_1} + e^{i\phi_2} \right|^2 = 2A^2(1 + \cos \Delta\phi), \quad (4.15)$$

where the phase difference between paths 1 and 2 is given by

$$\Delta\phi = \phi_1 - \phi_2 \approx \frac{2\pi xd}{\lambda L}. \quad (4.16)$$

The flux of particles at position x on the screen can thus be written as

$$N(x) = 4A^2 \cos^2 \left(\frac{\pi xd}{\lambda L} \right), \quad (4.17)$$

where I have used the trig identity $(1 + \cos x)/2 = \cos^2(x/2)$.

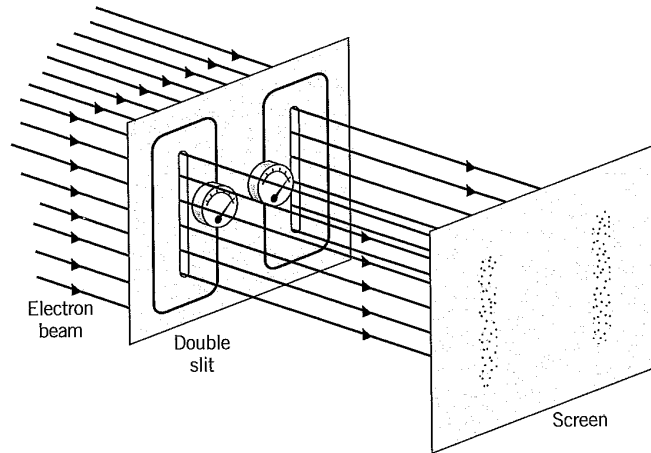


Figure 4.7: Double-slit which-way experiment. Each slit is surrounded by a wire loop connected to a meter to determine through which slit an electron passes. No interference fringes are observed on the screen.

Now suppose that we want to try to determine through which slit the electron passed. This could be done by introducing a wire loop around each slit that causes a meter to deflect each time a charged particle passes through the slit as depicted in Fig. 4.7. If we performed such an experiment we would find that the interference pattern no longer appears, but rather just a pattern of two peaks. By measuring through which slit the particle passes, we no longer have two possible paths that the particle can take to the screen, we have collapsed the possible paths to only one. This destroys the superposition of amplitudes in Eq. (4.15) required to obtain the double-slit interference pattern. This thought experiment nicely demonstrates the *principle of complementarity*. When we ask through which slit the particle passed, we are investigating the particle aspects of its behavior only, and thus cannot observe any of its wave nature (the interference pattern). Conversely, when we study the wave behavior, we cannot simultaneously observe the particle nature (the classical trajectory). The particle will behave as a particle or a wave, but we cannot observe both aspects of its behavior simultaneously.

4.3 Wave function

One major challenge to de Broglie's waves arises when one asks, "What is waving and what does the amplitude of the wave represent?" De Broglie interpreted his waves as "pilot waves" or "guiding waves" that direct the particle trajectory. This interpretation was further developed by David Bohm and gives an alternative formulation of quantum physics. However, the more



Figure 4.8: Max Born

standard interpretation of the de Broglie waves comes from Max Born, who published his interpretation of the wave function in 1926. The “state” of a quantum system is completely governed by its wave function $\psi(x, t)$ (assuming a particle confined to move in one dimension), which is called a *probability amplitude*. The probability to find the particle between x and $x + dx$ at time t is given by

$$P(x, t)dx = |\psi(x, t)|^2 dx. \quad (4.18)$$

This implies that if we know the wave function for a particle to be $\psi(x)$, to determine the probability to find this particle between $x = -a$ and $x = +a$, we must integrate each infinitesimal probability

$$P(-a < x < a, t) = \int_{-a}^{+a} |\psi(x, t)|^2 dx. \quad (4.19)$$

This is illustrated in Fig. 4.9, which shows a Gaussian probability distribution.

Note that this interpretation implies that the integral over all space of this probability density should give unity (the particle has to exist somewhere in space)

$$\int_{-\infty}^{\infty} P(x, t)dx = \int_{-\infty}^{\infty} |\psi(x, t)|^2 dx = 1. \quad (4.20)$$

Thus, for a single run of the experiment we cannot determine specifically where a particle will be detected, but we can use the wave function to predict the probability to find the particle at a point on the detection screen. In the next chapter we will discuss the mathematical framework for calculating the

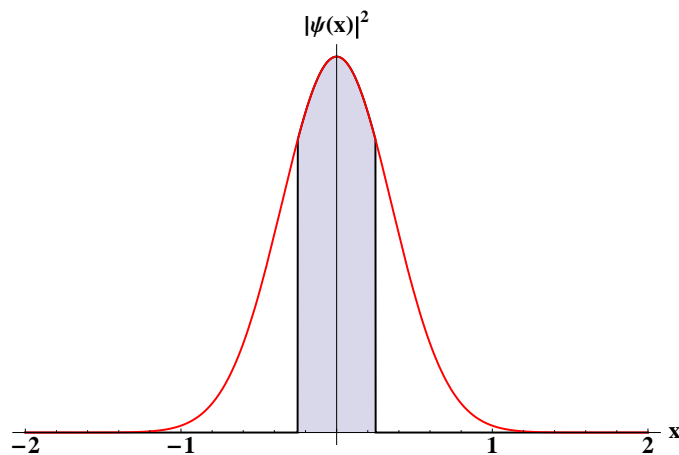


Figure 4.9: The modulus squared of the wave function $|\psi(x)|^2$ is interpreted as the probability density for the particle described by the wave function $\psi(x)$. The integral between two limits, chosen here to be $\pm a = \pm 0.25$, gives the probability of finding the particle in this region (at time t if there is a time dependence of the wave function).

wave amplitudes and develop a more rigorous definition of the probability density.

4.4 Uncertainty relations

A central aspect of the dual wave-particle nature of quantum systems is the indeterminism associated with measurement outcomes. This wave-particle duality is most pronounced when discussing the uncertainties associated with the simultaneous measurement of the position and momentum of a quantum particle. In classical physics, we think of uncertainty as a flaw in our measurement devices. For example, if we attempt to measure the position of a particle with respect to another particle using a ruler with millimeter scale divisions, we can at best quote the position to say the nearest half millimeter. The uncertainty in the position, which we denote by Δx , is limited by our measurement device. A further source of uncertainty in measurements arises from statistical fluctuations in the measurement process, for example, we might not quite line up the ruler origin at exactly the same point for repeated measurements. This type of random error can be eliminated by repeating the measurement many times and using the average value of the measurement outcomes and their standard deviation to estimate the true value of the position. Furthermore, if the particle is moving and we wanted to measure the position and momentum of the particle, there is nothing to stop us from doing both simultaneously to any level of precision.

However, in quantum physics there are inherent uncertainties associated with the values of measurements performed on quantum systems. The uncertainty principle (or Heisenberg uncertainty principle named after its discoverer) tells us that the product of uncertainties associated with position and momentum must be greater than or equal to the Planck constant divided by 4π , i.e.

$$\Delta x \Delta p_x \geq \frac{\hbar}{2}, \quad (4.21)$$

where $\hbar = h/2\pi$ as usual. We interpret this inequality by stating that if we try to measure both position and momentum simultaneously, the product of their uncertainties must be larger than a very small, but finite value. In other words, it is not possible to simultaneously determine the position and momentum of a quantum system with unlimited precision. This uncertainty principle in x and p_x can be extended to other measurement outcomes including the two other spatial-momentum directions (y, p_y and z, p_z) as well as other *complementary observables*, that is quantities that cannot be simultaneously determined to arbitrary precision (many, but not all, complementary observables turn out to be Fourier-transform pairs). For example, there is an uncertainty relation between energy and time

$$\Delta E \Delta t \geq \hbar. \quad (4.22)$$



Library of Congress

Figure 4.10: Werner Heisenberg

These uncertainty relations give a fundamental limit to the best that we can hope to do in determining measurement precision. We can do worse than these uncertainty relations, but nature sets the rules that we may do no better. This is a profound implication about our view of the natural world.

Taken to the extreme the uncertainty principle not only holds for measurement outcomes, but at a deeper level says for example that position and momentum cannot be simultaneously well-defined for a quantum system - a particle cannot have both a precise position in space and a precise direction of propagation. This latter statement refers directly to our notions of reality - does a particle really possess an exact position and momentum and we are simply ignorant of these qualities? Or do we only attribute these qualities of position and momentum after making a measurement on the system. It is the latter approach that is taken in quantum mechanics, which has far-reaching implications when one starts to think about ever larger quantum systems. We will discuss these issues in greater detail in future lectures, but I wanted to plant the seed for now.

The uncertainty principle arose from a different mathematical approach to quantum physics from the de Broglie-Schrödinger wave-function approach known as matrix mechanics. This method was developed by Werner Heisenberg, Max Born and Pascual Jordan at approximately the same time that Schrödinger developed his wave-mechanics approach to quantum physics (1925-1926). There was a brief period of confusion (1926-1927) during which two, seemingly unrelated approaches to quantum theory existed and gave identical predictions. However, this confusion was short lived and Schrödinger showed that indeed the two methods were mathematically equivalent. Due to the familiarity of physicists with the mathematical tools of wave motion compared with the mathematics of matrices, owing to the prevalence of wave phenomena in classical physics (light, sound, water, etc...), Schrödinger's approach was much more widely adopted. This is perhaps one reason why the wave approach is still the way quantum physics is introduced. To circumvent the difficulties associated with introducing the matrix mechanics formalism, which you will learn next year, we will discuss two examples from which the uncertainty relations arise naturally.

Uncertainty principle from a slit

Consider a beam of particles with well defined momentum traveling in the z direction as shown in Fig. 4.11. The de Broglie wavelength is well defined for such a system of particles owing to the well defined momentum. The amplitude associated with such a de Broglie wave is given by

$$\psi(x, y, z, t) = Ae^{i(p_z z - Et)/\hbar} \quad (4.23)$$

which is the equation for a plane wave traveling in the z direction with wavevector $k_z = p_z/\hbar$ and angular frequency $\omega = E/\hbar$. Note that the position of such a particle in the x and y directions is completely unknown ($\Delta x = \Delta y = \infty$) - the plane wave spreads infinitely in these directions.

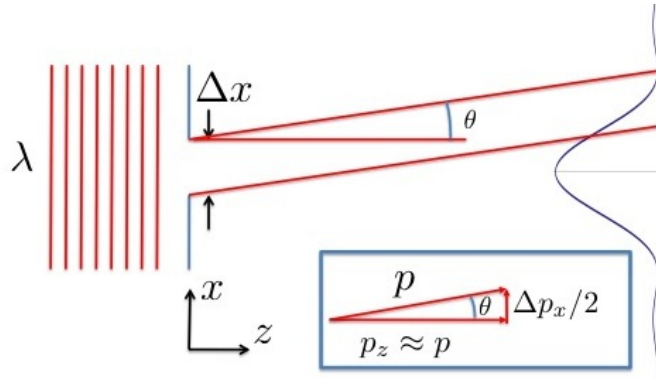


Figure 4.11: Single-slit diffraction as a source of uncertainty for transverse momentum. A plane wave traveling in the z direction is incident on the single slit of width Δx . Initially there is no uncertainty in the momentum components of the particle, $p_z = h/\lambda$ and $p_x = 0$, while the transverse position is completely uncertain since the plane wave is spread across all space. However, the slit localizes the particle to within its transverse width Δx , identified with the finite transverse position uncertainty. This will induce an uncertainty in the transverse momentum, which we estimate by considering the first-order diffraction minimum on either side of the peak. These occur when $\Delta x \sin \theta = \lambda/2$, using the edges of the slit as point sources. The inset shows the relationship between the scattered momentum vector p and its components, giving $\Delta p_x/2 \approx p \sin \theta$.

Furthermore, the uncertainty in the momentum for the particle is zero, that is the momentum is precisely defined. Now, by introducing a slit into the path of the quantum particle, we reduce the uncertainty in the particle transverse position, to the width of the slit. For simplicity, we will only discuss the x direction now, but a similar argument holds for the y direction as well. There should be a corresponding increase in the uncertainty in the transverse momentum to accompany this new localization of the particle.

To estimate the uncertainty in the transverse momentum, we can use our knowledge from classical wave optics about diffraction effects that arise from passing a wave through such a slit. We can approximate the spread in momentum by thinking about the first order diffraction minimum, which we can calculate by considering only the two end points of the slit as acting like a double slit. The angle for the first minimum occurs when

$$\Delta x \sin \theta = \frac{\lambda}{2}, \quad (4.24)$$

where θ is the angle from the z axis that the momentum is directed. This implies that

$$\Delta x = \frac{\lambda}{2 \sin \theta}. \quad (4.25)$$

The uncertainty in the transverse momentum is associated with the deflection angle experienced by the particle and can be determined from geometry as

$$\Delta p_x \approx 2p \sin \theta. \quad (4.26)$$

Note that the factor of 2 on the right hand side of Eq. (4.26) arises from considering the full transverse momentum uncertainty in the positive and negative directions. Multiplying Eqs. (4.25) and (4.26) together we arrive at the uncertainty relation for transverse position and momentum due to the wave nature of quantum systems

$$\Delta x \Delta p_x \approx \frac{\lambda}{2 \sin \theta} 2p \sin \theta = \lambda \frac{h}{\lambda} = h, \quad (4.27)$$

where we used the de Broglie relation $\lambda = h/p$.

Application of the uncertainty principle

The uncertainty principle can be used to calculate various quantities to give an order of magnitude estimate in quick calculations. For example, consider the energy associated with the ground state of a helium ion. First we assume that the electron is bound to the helium ion at a radius of approximately $a_0/2$, where $a_0 \approx 0.5\text{\AA}$ is the Bohr radius and the factor of $1/2$ arises from the stronger Coulomb attraction of the nucleus due to the additional proton in the nucleus. Then by assuming this orbital radius is the uncertainty in the radial position,

$$\Delta r \approx a_0/2, \quad (4.28)$$

the corresponding momentum uncertainty will be

$$\Delta p_r \approx 2\hbar/a_0, \quad (4.29)$$

from the uncertainty relation $\Delta r \Delta p_r \approx \hbar$. The energy associated with this confined particle can be estimated by taking the non-relativistic kinetic energy associated with the particle bouncing back and forth inside the ion with momentum $p_r \approx \Delta p_r$, giving

$$\begin{aligned} E_{\text{bind}} &\approx \frac{\Delta p_r^2}{2m} \approx 2 \frac{\hbar^2}{ma_0^2} = 2 \frac{1}{mc^2} \left(\frac{hc}{2\pi a_0} \right)^2 \\ &\approx 2 \frac{1}{0.5 \text{ MeV}} \left(\frac{1240 \text{ eV nm}}{2\pi(0.05 \text{ nm})} \right)^2 \\ &\approx 62 \text{ eV}, \end{aligned} \quad (4.30)$$

which is surprisingly close to the value predicted by the Bohr model, $E = Z^2 E_1 = 2^2 \times 13.6 \text{ eV} \approx 54.4 \text{ eV}$.

4.5 Wave packets

A pure sine wave has a well-defined wavelength and thus frequency (energy) and momentum, but is completely delocalized in space, spreading infinitely throughout space. The same holds for plane waves as discussed in the previous section. A classical particle, on the other hand is completely localized in space, has a well-defined position and therefore trajectory. An electron bound to an atom is localized in position to within an uncertainty on the order of the atomic diameter (given by twice the Bohr radius for example), but its precise position within the atom is not well defined. To describe such “quasi-localized” waves, physicists have at their disposal the concept of *wave packets*. A wave packet can be considered to be the superposition of many waves that interfere constructively in the vicinity of the particle, giving a large amplitude where the particle is expected to be found, and interfere destructively far from where the particle is predicted to be found.

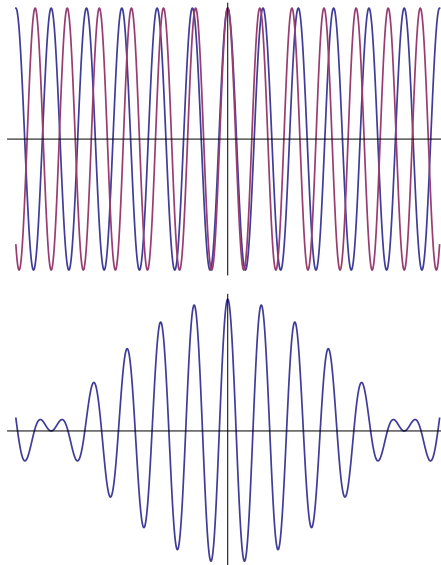


Figure 4.12: Two cosine waves with slightly different wavelengths (top) add constructively in superposition near zero displacement (bottom), but destructively further away. This leads to a beat pattern.

In one dimension, we can add two sine waves with different, but nearly equal, wave vectors, k_1 and k_2 , which leads to a beat pattern with a spatial localization for part of the wave depicted in Fig. 4.12. The associated wave

is given by

$$\psi_2(x) = A(\sin(k_1x) + \sin(k_2x)), \quad (4.31)$$

where we have assumed equal amplitudes for both wave vector components. By adding more waves to this superposition, say N in total, with appropriate wave vectors and relative phases, we can create an increasingly localized wave packet as shown in Fig. 4.13.

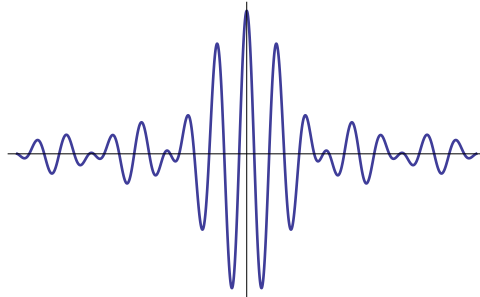


Figure 4.13: Wave packet constructed from ten different cosines, each with slightly different wavelengths.

The corresponding wave can be written as

$$\psi_N(x) = A \sum_{m=1}^N \sin(k_m x), \quad (4.32)$$

where again we assumed equal phases and amplitudes for each component. In general, we can have different amplitudes and phases for each wave vector component and the sum can be infinite, giving an amplitude

$$\psi(x) = \sum_{m=1}^{\infty} A_m \exp [i(k_m x + \phi_m)], \quad (4.33)$$

where we have used complex notation for our waves. This is nothing other than a Fourier series. It is a well-known mathematical result that any periodic function can be decomposed into a sum of sine and cosine functions (or equivalently complex exponentials thanks to the Cauchy relation $e^{i\theta} = \cos \theta + i \sin \theta$) with appropriately chosen amplitudes and phases.

We are not restricted to a discrete sum of possible wave vectors and we can choose a continuous distribution of wave vectors to include in our wave packet. In this situation, the sum in Eq. (4.33) can be replaced by an integral

$$\psi(x) = \int_{-\infty}^{\infty} A(k) e^{ikx} dk. \quad (4.34)$$

Here, the amplitude $A(k)$ is taken to be complex to include both the amplitude and phase differences between different wave vector components that make up the wave packet. Let us start with a Gaussian distribution of wave vectors

$$A_{\text{Gauss}}(k) = A_0 \exp\left(-\frac{k^2}{2\Delta k^2}\right), \quad (4.35)$$

where A_0 is a normalization constant, and $\Delta k/\sqrt{2}$ is the full $1/e^{1/2}$ width of the probability distribution, (which we will see corresponds to the uncertainty in the momentum). This probability amplitude $A(k)$, and its corresponding probability distribution $p(k) = |A(k)|^2$ are shown in Fig. 4.14.

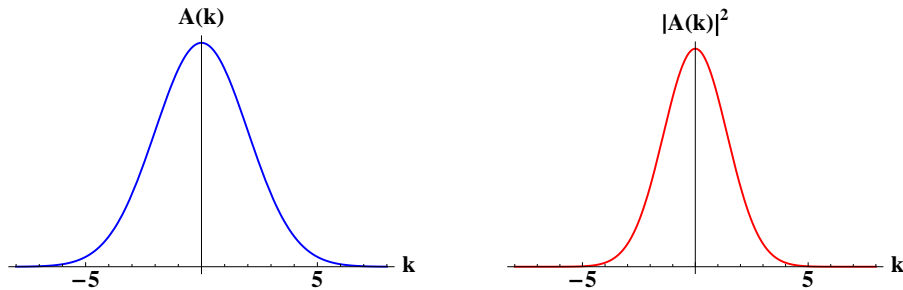


Figure 4.14: Gaussian wave vector (k) probability amplitude $A(k)$ (left) and corresponding probability distribution $p(k) = |A(k)|^2$ (right). Note that by squaring the amplitude to get the probability distribution the width becomes smaller by a factor of $1/\sqrt{2}$.

Note that the uncertainty in the momentum of a particle with such a wave vector distribution is given by \hbar times the width of the wave vector *probability distribution* (not the probability amplitude), that is the width of $P(k) = |A(k)|^2$, which is just $\Delta k/\sqrt{2}$ for a Gaussian distribution of the form in Eq. (4.35). The factor of $1/\sqrt{2}$ comes from the fact that the width is associated with the full $1/e^{1/2}$ width of the probability distribution (not the amplitude). In other words, the momentum uncertainty for a particle described by the wave vector distribution in Eq. (4.35) is

$$\Delta p = \frac{\hbar \Delta k}{\sqrt{2}}. \quad (4.36)$$

The corresponding wave packet in the spatial domain, $\psi(x)$, is

$$\begin{aligned} \psi_{\text{Gauss}}(x) &= \int_{-\infty}^{\infty} A_0 \exp\left(-\frac{k^2}{2\Delta k^2}\right) e^{ikx} dk \\ &= A_0 \sqrt{2\pi} \Delta k \exp\left(-\frac{x^2 \Delta k^2}{2}\right). \end{aligned} \quad (4.37)$$

The wave packet amplitude and probability distribution corresponding to the momentum distribution in Fig 4.14 is shown in Fig. 4.15 below.

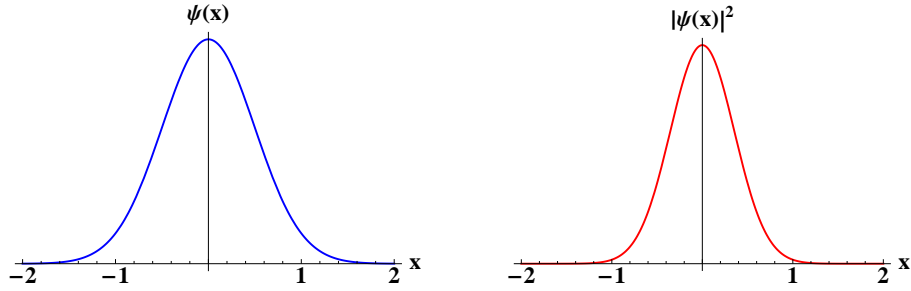


Figure 4.15: Gaussian wave packet probability amplitude $\psi(x)$ (left) and corresponding probability distribution $P(x) = |\psi(x)|^2$ (right). The width of the probability distribution, corresponding to the extent the particle is localized, is inversely proportional to the width of the momentum probability distribution, that is, $\Delta x \approx \hbar/\Delta p$. So a broader momentum distribution implies a narrower position distribution and thus a more localized (classical-like) wave packet.

The integral in Eq. (4.37) can be found from the following definite integral

$$\int_{-\infty}^{\infty} \exp(-ax^2 + bx) = \sqrt{\frac{\pi}{a}} \exp\left(\frac{b^2}{4a}\right). \quad (4.38)$$

Similar, to the wave vector case, the uncertainty in the position for a particle with the corresponding Gaussian wave packet of Eq. (4.37) can be read off

$$\Delta x = \frac{1}{\sqrt{2}\Delta k}. \quad (4.39)$$

Multiplying out the uncertainties in position and momentum we see that a Gaussian wave packet is a minimal uncertainty state, that is, the uncertainty in the momentum and position saturate the Heisenberg limit

$$\Delta x \Delta p = \frac{\hbar}{2}. \quad (4.40)$$